Disordered AlAs wires: Temperature-dependent resonance areas within the Fermi-liquid paradigm

J. Moser,[1,2,*] S. Roddaro,[2] D. Schuh,[1] M. Bichler,[1] V. Pellegrini,[2] and M. Grayson[1]
[1]*Walter Schottky Institut, Technische Universität München, D-85748 Garching, Germany*
[2]*NEST-CNR-INFM, Scuola Normale Superiore, I-56126 Pisa, Italy*
(Received 22 September 2006; published 10 November 2006)

AlAs cleaved-edge overgrown quantum wires near pinch-off reveal conductance resonances with an unconventional dependence on temperature T. The resonance areas decrease with reduced T consistent with classical Coulomb blockade (CB) in a single dot, but then become rapidly smaller below a crossover T_X. Though resembling Luttinger liquid behavior below the crossover, the anomalous T dependence including the crossover fit quantitatively to a classical-to-stochastic CB transition, whereby stochastic multidot CB sets in at low temperatures. Conductance at finite bias resembles a depinned charge density wave as expected for a chain of disorder induced dots. These studies highlight the applicability of the Fermi liquid paradigm to the description of disordered heavy-mass quantum wires.

DOI: 10.1103/PhysRevB.74.193307 PACS number(s): 73.21.Hb, 73.20.Mf, 73.23.Hk

Quantum wires are interesting one-dimensional (1D) systems for the study of electronic correlations at the heart of the Luttinger liquid (LL) model.[1] In this formalism, a correlation-induced pseudogap in the tunneling density of states opens up at the Fermi level at low temperature T. As evidence for such behavior, recent transport experiments in GaAs cleaved-edge overgrown wires[2] and single-wall carbon nanotubes[3] yield conductance resonances with vanishing areas as T is lowered.

Heavier mass m^* 1D wire systems like AlAs would have a lower kinetic energy E_F than their GaAs counterpart at the same density n_{1D}, resulting in an even larger role for correlations. However disorder will also become more relevant with the reduced kinetic energy, and can lead to strongly T-dependent resonances areas when two or more localized zero-dimensional (0D) charge islands are in series. For such heavy mass disordered systems, it is essential to clearly identify whether correlations or disorder are responsible for the resulting behavior. It is worth noting that disorder may also play a larger role in carbon nanotubes than originally believed.[4] AlAs 1D systems are important to study in their own right, as they host two degenerate X-valleys of electrons,[5] and the double X-valley degeneracy $g_v=2$ reduces the kinetic energy at a given density by yet another factor of four $E_F=\frac{\hbar^2}{2m^*}\left(\frac{\pi n_{1D}}{g_s g_v}\right)^2$ relative to GaAs, where g_s is the spin degeneracy.

In this paper, disordered heavy-mass AlAs wires[5] fabricated by cleaved-edge overgrowth (CEO) are studied in the Coulomb blockade (CB) regime. We report low-T differential conductance measurements as a function of source-drain dc bias V_{SD}, and top gate bias V_{GD} which tunes the wire density. We observe CB resonances which become vanishingly small below an intermediate crossover T_X and find that the Fermi liquid approach proposed by Ruzin *et al.*[6] for a series of weakly coupled dots is able to explain the existence of this crossover as well as the CB resonance line shapes on both sides of the crossover. By fitting the T dependence of the resonance according to Ref. 6, we determine the capacitances of the two limiting dots. We complete our study by considering the differential conductance dI/dV_{SD} at finite V_{SD}. Outside the CB gap, dI/dV_{SD} shows a single maximum followed by a monotonically increasing background, consistent with a charge density wave pinned in a chain of dots.[7]

The quantum wire samples are fabricated from a 150 Å wide, modulation-doped AlAs two-dimensional electron system (2DES) sandwiched between two AlGaAs spacers and grown on a (001) GaAs substrate (see inset to Fig. 1). The substrate is cleaved *in-situ* at the perpendicular (110) plane and overgrown with another modulation-doped barrier.[5] Electrons in the two degenerate X-valleys accumulate along the cleaved edge of the 2DES and form the doubly valley-degenerate 1D system. A 1 μm wide metal gate on the substrate depletes the 2DES underneath and varies the wire density in the segment located below it. The 2DES regions on each side of the gate serve as ohmic contacts, and conductance measurements are performed in a two-point configuration using $V_{ac}\simeq 10\ \mu V < k_B T$ and standard lock-in techniques. The effective mass in the direction of the wire is $m^*=0.33m_0$ in units of the free-electron mass. Samples are cooled down in a dilution refrigerator with an electron base temperature $T=100$ mK. The substrate and the cleaved edge are illuminated at 10 K with two infrared light-emitting diodes.

Figure 1 depicts combs of conductance resonances at $T=100$ mK as the gate bias V_{GD} is scanned past the pinch-off threshold. The first V_{GD} sweep after illumination and at base T yields quasiperiodic resonances. Upon sweeping V_{GD} repeatedly in the same direction some resonances appear to be quite robust while others shift. By the fourth gate sweep most resonances have vanished and those remaining are lumped close to threshold.

We interpret this behavior as Coulomb blockade (CB) in a disorder potential. As the wire is depleted, the disorder potential isolates 0D islands of electrons throughout the wire, whose capacitance defines a charging energy which periodically blocks single electron transport. Presumably, cycling V_{GD} affects the distribution of ionized dopants underneath the gate,[8] inducing variations in the potential background seen by the wire at each cycle. However by narrowing the gate bias window it is possible to preserve one resonance

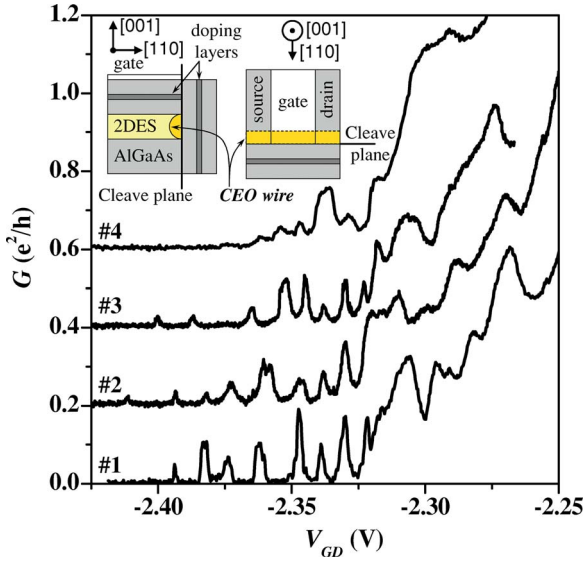

FIG. 1. (Color online) Conductance G vs gate bias V_{GD} for several V_{GD} sweeps in the positive-voltage direction at a base electron temperature $T=100$ mK. Beyond the fourth sweep it becomes increasingly difficult to resolve resonances. Each trace is offset by $0.2e^2/h$ for clarity. Inset: schematic of the sample.

upon multiple V_{GD} cycles and perform a systematic study of it, as we now demonstrate.

We study two resonances **A** and **B** in detail. Each is observed in a separate cooldown, and is well isolated and located at a similar V_{GD} away from threshold. Figure 2(a) illustrates the influence of T on resonance **A**, and Fig. 2(b) summarizes the T dependence of the peak conductance G_{max} and of the resonance area $\mathcal{A}$ for **A** and **B**. Two distinct T regimes are apparent in Fig. 2(b): G_{max} is weakly T dependent above 250 mK, then sharply falls off at lower T. $\mathcal{A}(T)$ is linear for $T>250$ mK but drops rapidly for $T<250$ mK. At base T both resonances resolve into a striking triple-peak [inset to Fig. 2(a)].

To explain these observations, we recall that for classical CB a single dot limits conduction, where k_BT is larger than the energy level spacing Δ in the dot ($k_BT>\Delta$), and the only relevant energy scale is the dot charging energy e^2/C. In this regime, the peak conductance should be constant and the linewidth linear in T,[9] suggesting that the data in Fig. 2(b) at higher T is consistent with classical CB. Presumably, the large m^* in AlAs reduces Δ and makes it difficult to reach the *quantum* CB regime where $k_BT<\Delta$.

The reduced resonance strength at lower T suggests the onset of an additional current limiting mechanism. This regime has been addressed theoretically by Ruzin *et al.*[6] assuming transport limited by two asymmetric quantum dots in series, a regime known as stochastic CB. The model in Ref. 6 is again classical ($k_BT>\Delta_1,\Delta_2$) and considers the case where tunneling is incoherent and the potential on each dot v_1,v_2 is tuned by a common gate $\Delta v_1=\Delta v_2=\Delta V_{GD}$ [see inset to Fig. 2(b)]. Following the notation of Ref. 6, individual dots 1 and 2 are characterized by their capacitances to the gate C_1 and C_2. The interdot capacitance C' as well as the capacitance between each dot and either source or drain C is assumed in the model to be zero $C=C'=0$, such that the total

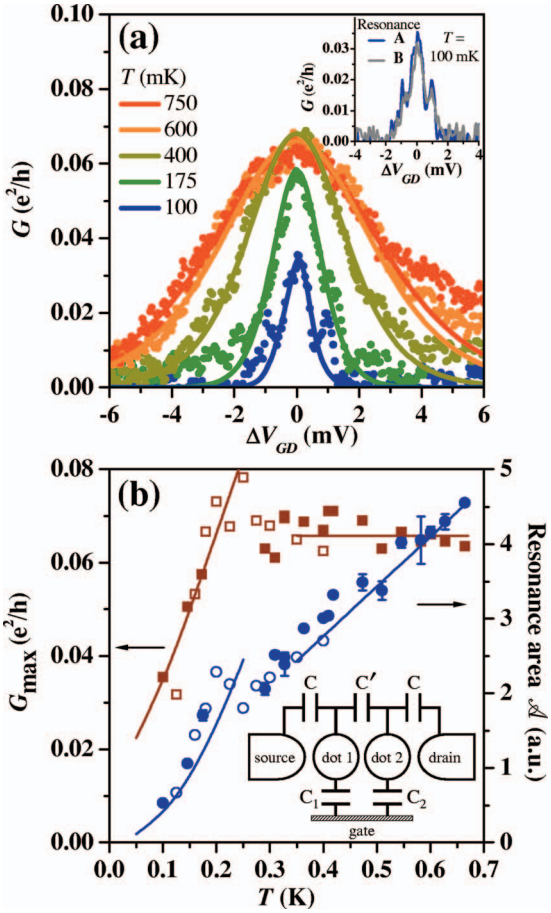

FIG. 2. (Color) (a) Evolution of a resonance **A** with temperature T. Curve fits of the model of Ref. 6 for two asymmetric dots in series are shown assuming capacitances described in the text. Resonances **A** and **B** in the inset share a similar triple-peak structure at base T. (b) Conductance peak G_{max} (red) and resonance area $\mathcal{A}$ (blue) as a function of T. Filled (hollow) symbols correspond to resonance **A** (**B**). $\mathcal{A}$ is twice the integrated area of the left half of the resonance; error bars quantify the left-right asymmetry at higher T, and correspond to $\pm|\mathcal{A}-\text{full area}|/2$. Lines are fit to the model of Ref. 6.

capacitance of dot i is $C_i^{tot}=C_i$. Transport through the double dot structure occurs only when both dots have an available level in their energy spectra within k_BT of the Fermi energy. In the case of strongly asymmetric dots, e.g., $C_1^{tot}\ll C_2^{tot}$, the large difference in the addition spectrum spacings $e^2/C_1^{tot}\gg e^2/C_2^{tot}$ makes this condition increasingly difficult to meet at low T, leading to vanishing resonances characteristic of stochastic CB. On the other hand, for $k_BT>e^2/C_2^{tot}$, the model in Ref. 6 explains that the discreetness of the addition energy spectrum of dot 2 is no longer relevant and transport is dominated by the charging of the single dot 1, recovering the high T classical CB limit observed experimentally.

For quantitative comparison, we deduce various capacitances from the data according to the model in the Fig. 2(b) inset, allowing for finite C',C. The typical resonance spacing $\Delta V_{GD}\simeq 10$ mV (Ref. 10) is determined by the smallest gate-dot capacitance $C_1\ll C_2$, whereby $C_1=e/\Delta V_{GD}$

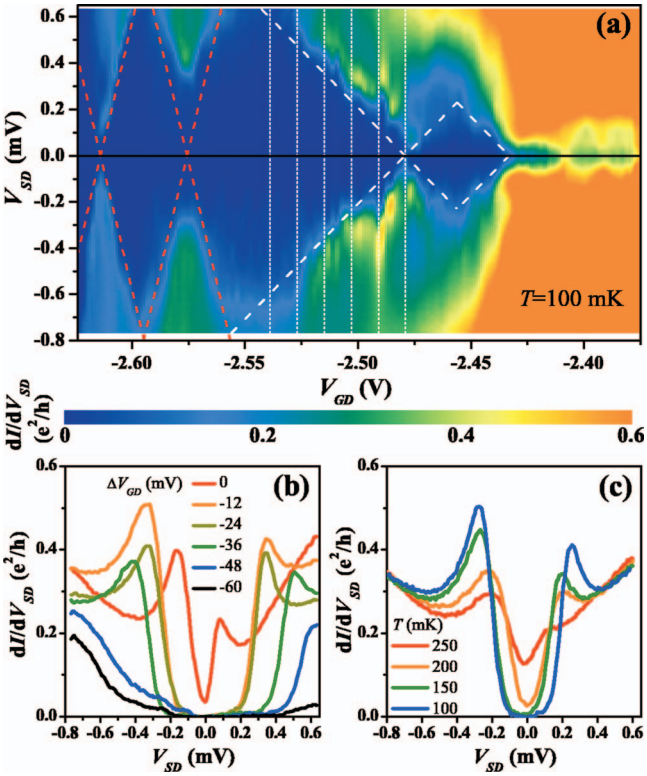

FIG. 3. (Color) (a) Differential conductance dI/dV_{SD} as a function of source-drain dc bias V_{SD} and gate bias V_{GD} at $T=100$ mK. Diamonds are highlighted. (b) Subset showing traces at fixed V_{GD} indicated by the vertical dashed lines in (a). The conductance at $\Delta V_{\mathrm{GD}}=0$ and $V_{\mathrm{SD}}=0$ corresponds to the maximum of a resonance peak. (c) Temperature dependence of dI/dV_{SD} at fixed $V_{\mathrm{GD}}\sim 50$ mV from pinch-off, taken from a different dataset.

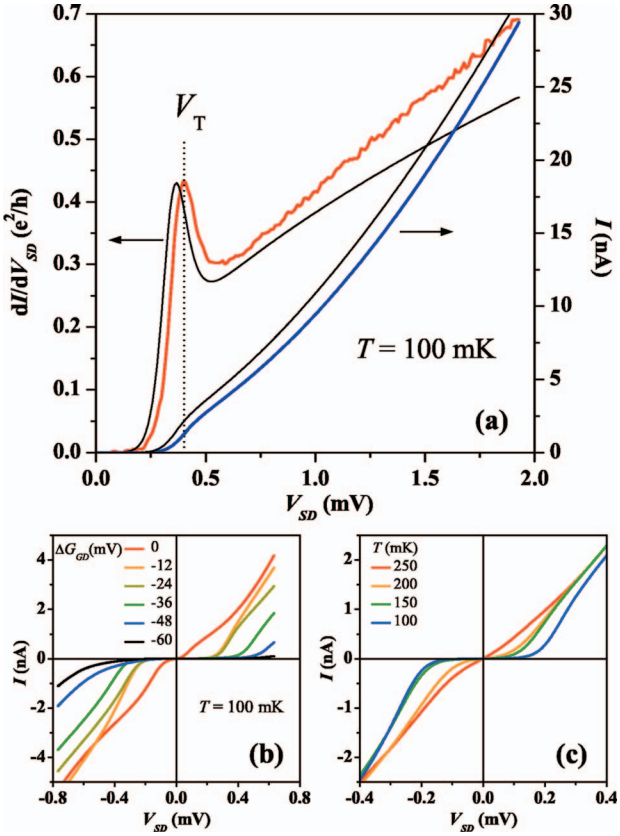

FIG. 4. (Color) (a) Typical dI/dV_{SD} (V_{SD}) and integrated current $I(V_{\mathrm{SD}})$. Theoretical $I(V_{\mathrm{SD}})$ from Ref. 7 and corresponding $dI/dV_{\mathrm{SD}}(V_{\mathrm{SD}})$ are plotted as thin curves. (b) Integrated $I(V_{\mathrm{SD}})$ from traces of Fig. 3(b). (c) Temperature dependence of $I(V_{\mathrm{SD}})$ after integration of dI/dV_{SD} in Fig. 3(c).

$\simeq 0.016$ fF. The thermal linewidth[9] $4.4k_BT$ of the high temperature resonances yields the ratio $\partial E_F/\partial V_{\mathrm{GD}}=eC_1/C_1^{\mathrm{tot}}=40$ meV/V from which $C_1^{\mathrm{tot}}=0.4$ fF ($e^2/C_1^{\mathrm{tot}}\simeq 400$ μeV). Following Ref. 6 we now set charging energy of the larger dot equal to the classical-to-stochastic crossover energy scale $e^2/C_2^{\mathrm{tot}}=k_BT_X=21$ μeV ($C_2^{\mathrm{tot}}=7.6$ fF), with $T_X=250$ mK.[11] We can adapt the analytical expression from Ref. 6 for the conductance line shape provided that each dot voltage now scales as $v_i=(C_i/C_i^{\mathrm{tot}})V_{\mathrm{GD}}$. Assuming that the interdot capacitance C' is small compared to the other capacitances, the complete set of calculated resonance line shapes is plotted in Fig. 2(a), with the solid lines in Fig. 2(b) representing the calculated peak conductances and areas. This simple model is found to capture the experimental line-shape evolution as a function of T surprisingly well. We verified that the line-shape
evolution with T is independent of C_2 provided that $C_1^{\mathrm{tot}}\gg C_2^{\mathrm{tot}}>C_2$. The triple-peak structure at 100 mK shown in the inset to Fig. 2(a) might arise from the finite interdot coupling capacitance C' which is expected to play a role at very low T;[6,12] or alternatively from a breaking of the in-plane valley degeneracy as observed in single-walled carbon nanotube dots.[13] However in both cases a twinning of resonances is expected, instead of the observed triad.

Having demonstrated evidence of a classical-to-stochastic CB crossover in AlAs disordered wires, we now focus on the finite source-drain bias dependence and nonlinear conductance. The color plot in Fig. 3(a) reports the differential conductance dI/dV_{SD} as a function of V_{GD} and V_{SD} at $T=100$ mK. Data are collected by sweeping V_{SD} and stepping V_{GD}. All features evolve smoothly without any significant trapped charge events. CB diamonds defined as regions of vanishing conductance are highlighted with dashed lines. Note that the vanishingly small resonances at $V_{\mathrm{SD}}=0$ are not visible on this color scale. Near threshold CB diamonds highlighted in white are visible. Additional diamonds with a steeper $dV_{\mathrm{GD}}/dV_{\mathrm{SD}}$ slope are observed at more negative V_{GD} values (red dashed lines). Figure 3(b) shows several dI/dV_{SD} vs V_{SD} traces at fixed V_{GD} as indicated by the vertical dashed lines in Fig. 3(a): a gap structure centered at $V_{\mathrm{SD}}=0$ develops beyond pinch-off as T is lowered [Fig. 3(c)]. Similar nonlinear features are observed for three separate cool downs of the same sample (data not shown). Note that unlike standard CB, the CB diamonds here meet at a saddle point: zero-bias resonance maxima in dI/dV vs V_{GD} (i.e., Figs. 1 and 2) corresponds to a strong minima in dI/dV vs V_{SD} [Fig. 3(b)] similar to observations in Si split-gate wires.[15]

The differential conductance dI/dV_{SD} outside of the gaps in Fig. 3 also displays unconventional features. The conductance of Fig. 3(b) shows a single peak flanked with a wing of monotonically increasing background conductance. This contrasts the standard CB behavior which would show a se-

ries of peaks outside the gap region. This first peak also shows the T broadening expected for CB features [Fig. 3(c)], but the wings at higher voltage show no obvious T dependence.

The finite bias peak and curious saddle point in the CB may be explained in terms of models which take into account interactions with the localized dot charge. One possibity is a Fermi-edge singularity (FES) in the tunneling density of states of the wire,[14] whereby an electron tunneling into a dot is in resonance with the hole left in the wire. However an alternate scenario involving a pinned density wave, as first proposed in Ref. 15, would more logically extend from the observed stochastic CB behavior at low energies. This effect is more easily recognized if the dI/dV_{SD} data of Figs. 3(b) and 3(c) are integrated to give $I-V_{SD}$ as shown in Figs. 4(b) and 4(c). Figure 4(a) magnifies a single dI/dV_{SD} curve to reveal a steplike current onset outside of the CB region. We can now identify the peak in dI/dV_{SD} in Fig. 4(a) as a threshold voltage V_T at which point the current is at the center of its steplike rise, and the charge flow becomes depinned. Reference 7 provides a quantitative description of how a chain of coupled dots in series can support current flow in the form of charge solitons, so for comparison we plot a theoretical $I-V_{SD}$ and its derivative taken from Ref. 7 in Fig. 4(a) along with the experimental data. The curve shown represents a chain of dots with equal interdot capacitances $C=1$ fF about a factor of 5 larger than the value in the present experiment. Reference 7 also predicts that the conductance threshold $V_T(V_{GD})$ resembles Coulomb diamonds that do not close, as observed here in experiment. In this case, the flow of charge density through the chain of quantum dots is pinned by the CB gap of the dot with the smallest capacitance, and outside of this gap the charge flows as a soliton wave through a chain of dots.

In summary, we have provided evidence that the crossover behavior and vanishing resonances at low T in disordered AlAs CEO wires are not explainable with the Luttinger liquid formalism, but rather with transport across several asymmetric quantum dots in series connected to Fermi liquid leads. At high T one resonant state dominates yielding classical CB, then there is a transition to a low-T stochastic CB when two asymmetric resonances limit the conduction. Finite bias differential conductance reveals a conductance threshold outside the Coulomb diamond which is suggestive of a charge soliton in a chain of coupled quantum dots. This conductance threshold outside of the CB gap resembles early results in heavy-electron mass disordered Si wires[15] as well as recent results in disordered long GaAs split gate wires.[16] It is also reminiscent of the conduction through split-gate constrictions in the quantum Hall regime at finite bias[17] suggesting that our experimental observations in AlAs may be important for the interpretation of other 1D systems.

The authors thank J. Weis, T. Giamarchi, Y. Meir, D. Goldhaber-Gordon, and G. Abstreiter for stimulating discussions. The authors gratefully acknowledge support from the COLLECT EC-Research Training Network, HPRN-CT-2002-00291, German BmBF Grant No. 01 BM 470, and FIRB "Nanoelettronica."

*Electronic address: moser@wsi.tu-muenchen.de

[1] For a review, see T. Giamarchi, *Quantum Physics in One Dimension* (Oxford University Press, Oxford).
[2] O. M. Auslaender, A. Yacoby, R. de Picciotto, K. W. Baldwin, L. N. Pfeiffer, and K. W. West, Phys. Rev. Lett. **84**, 1764 (2000).
[3] H. W. Ch. Postma, T. Teepen, Z. Yao, M. Grifoni, and C. Dekker, Science **293**, 76 (2001).
[4] Y. Fan, B. R. Goldsmith, and P. G. Collins, Nat. Mater. **4**, 906 (2005).
[5] J. Moser, T. Zibold, S. Roddaro, D. Schuh, M. Bichler, F. Ertl, G. Abstreiter, V. Pellegrini, and M. Grayson, Appl. Phys. Lett. **87**, 052101 (2005).
[6] I. M. Ruzin, V. Chandrasekhar, E. I. Levin, and L. I. Glazman, Phys. Rev. B **45**, 13469 (1992).
[7] N. S. Bakhvalov, G. S. Kazacha, K. K. Likharev, and S. I. Serdyukova, Sov. Phys. JETP **68**, 581 (1989).
[8] J. H. Davis, Semicond. Sci. Technol. **3**, 995 (1988).
[9] I. O. Kulik and R. I. Shekhter, Zh. Eksp. Teor. Fiz. **68**, 623 (1975) [Sov. Phys. JETP **41**, 308 (1975)]; E. B. Foxman, U. Meirav, P. L. McEuen, M. A. Kastner, O. Klein, P. A. Belk, D. M. Abusch, and S. J. Wind, Phys. Rev. B **50**, 14193 (1994).
[10] This value was measured as the distance between resonance **A** and its immediate neighbor. This also agrees with data in Fig. 1.
[11] The dot length L can be extracted by fitting C_1 to an electrostatic model for a cylinder-shaped dot $C_1 \simeq 2\pi\epsilon \ln(2d/R) \times L$, where $\epsilon = 12.5\epsilon_0$ is the dielectric constant of AlGaAs, $d=380$ nm is the gate-dot distance and $R=7.5$ nm is the dot radius, yielding $L \simeq 100$ nm.
[12] K. A. Matveev, L. I. Glazman, and H. U. Baranger, Phys. Rev. B **54**, 5637 (1996).
[13] W. Liang, M. Bockrath, and H. Park, Phys. Rev. Lett. **88**, 126801 (2002).
[14] D. A. Abanin and L. S. Levitov, Phys. Rev. Lett. **94**, 186803 (2005); K. A. Matveev and A. I. Larkin, Phys. Rev. B **46**, 15337 (1992).
[15] S. B. Field, M. A. Kastner, U. Meirav, J. H. F. Scott-Thomas, D. A. Antoniadis, H. I. Smith, and S. J. Wind, Phys. Rev. B **42**, 3523 (1990).
[16] T. Morimoto, M. Henmi, R. Naito, K. Tsubaki, N. Aoki, J. P. Bird, and Y. Ochiai, Phys. Rev. Lett. **97**, 096801 (2006).
[17] S. Roddaro, V. Pellegrini, F. Beltram, L. N. Pfeiffer, and K. W. West, Phys. Rev. Lett. **95**, 156804 (2005).